Revisiting the Koyna-Warna seismic zone: strain budget, present-day potential and associated hazard

Anup K. Sutar ⬤ · Sukanta Roy · V. M. Tiwari

Abstract The Koyna-Warna region in western India is well known around the globe for recurrent reservoir-triggered seismicity soon after the impoundment of the Koyna and Warna reservoirs. The seismicity pattern delineates two distinct seismic zones, Koyna Seismic Zone (KSZ) and Warna Seismic Zone (WSZ). To understand the seismic potential of the region, we estimated the strain budget by analysing the published GPS velocities and earthquake catalogue of the region. Although the KSZ and WSZ are separated by ~25 km only, the rate of strain accumulation in the former (2.55E+16 Nm/year) is estimated to be ~11 times larger when compared to the latter (2.29E+15 Nm/year). However, KSZ releases only ~20% of the accumulated energy per year, whereas, WSZ releases most of the accumulated energy in the form of earthquakes. Best fitting elastic dislocation model for KSZ also shows a left lateral slip of 0.8 mm/year and the fault plane dips at ~77° in NW direction. The distribution of strain accumulation and release rates in the two regions may be attributed to significant spatial variability in the medium properties such as density, elastic constants and fracture density. This proposition is supported by other geophysical studies in the region. A density model constructed from Airborne Gravity Gradiometry (AGG) data also shows relatively higher average density for KSZ compared to the WSZ. The strain budget of the region suggests that the earthquake activity in KSZ may continue for a longer time whereas it may diminish in the WSZ in the near future. Based on the gross strain estimates, the KSZ has accumulated enough strain post the 1967 M6.3 Koyna earthquake to generate an event of $M_w5.8$, provided the accumulated strain is released in a single event. The seismic hazard scenario in terms of peak ground acceleration (PGA) due to a potential $M_w5.8$ event is estimated using the stochastic simulation (SS) technique. The simulated PGA at a radial distance of ~40km from the source zone is estimated to range between 0.09 and 0.26g with an expected intensity of V–VII.

1 Introduction

The Koyna-Warna region located in the western part of the Deccan Traps province is a classical site of reservoir triggered seismicity since the impoundment of the Shivaji Sagar reservoir in 1962 (Fig. 1). The site was earlier considered aseismic and placed in the seismic zone '0' in the seismic zoning map of India (IS 1893–1962). During 1954, the Koyna hydroelectric project was taken up and construction of a dam on the Koyna River, near the Koynanagar town in Satara district, was

A. K. Sutar (✉) · S. Roy
Ministry of Earth Sciences, Borehole Geophysics Research Laboratory, Karad, India
e-mail: anupseismo@gmail.com

V. M. Tiwari
CSIR-National Geophysical Research Institute, Hyderabad, India

planned. The impoundment of the Shivaji Sagar reservoir in 1962 led to the occurrence of frequent low-magnitude earthquakes in the vicinity of the dam, culminating in the occurrence of the 1967 M6.3 Koyna earthquake (Guha et al. 1968; Narain and Gupta 1968; Rastogi et al. 1997). The 1967 M6.3 Koyna earthquake is the largest triggered earthquake in recorded history and calls for appropriate seismic hazard assessment for this region. After the 1967 M6.3 event, the seismic potential of the region was re-evaluated and the region was placed in the seismic zone IV in the seismic zoning map of India (IS 1893– 1962 (revised in 1966, 1970); BIS 2002). The M6.3 earthquake, with an observed maximum intensity of VIII in the MM scale near the epicentral zone, devastated the Koynanagar town causing nearly 200 deaths, injuring over 2000 people and rendering about 50,000 people homeless (Gupta et al. 1969).

Although the study region was considered aseismic before the impoundment of the Koyna dam, analysis of records collected by a single seismograph at Poona (Pune), located ~130 km NNE of Koyna and operational since 1950 found that infrequent low-magnitude earthquakes had occurred in the Koyna region prior to the construction of the dam (Milne 1911). Guha et al. (1968) have also reported ~20 strong earthquakes that occurred in the western margin of Indian peninsula, including the Koyna region, during 1594–1967. The catalogue of destructive earthquakes (7 to 1899 A.D.) compiled by Milne (Milne 1911) has reported as many as three destructive earthquakes in the Deccan region and the Koyna event of 1967 is one of them. Thus, evidence of infrequent seismic activity of the region can be found in the larger region surrounding Koynanagar in the Deccan Traps province, but the events do not result in marked structural changes of surface geological formations (Guha et al. 1968). The Donichawadi fissure zone, a ~200-m-wide zone of surface fissures mapped for a length of about 4 km along the NNE-SSW direction by the Geological Survey of India (GSI) in the wake of the 1967 Koyna earthquake remains the only record of surface expression in the region (GSI 1968).

In 1985, a new reservoir was constructed on the Warna River, ~25 km to the south of the Koyna dam (Fig. 1). The impoundment of the Warna reservoir in 1987 likely resulted in migration of the seismic activity in the region towards the south of the Warna River (Rastogi et al. 1997; Gupta 2017). The Koyna and Warna reservoirs seismic activity has continued for a few decades after their impoundment and are notable exceptions, which clearly pose continuing seismic hazard that is worth probing. In the present study, the persistent question regarding the recurrent seismicity in the Koyna-Warna region is investigated using present-day geodetic measurements as well as recorded recent seismicity of in the region. An evaluation of the expected maximum potential event in the region and simulation of the hazard scenario in terms of PGA has also been attempted.

2 Geologic and tectonic setting of the study area

The Koyna-Warna region is located on the Western Ghats escarpment, a steep, seaward-facing geodynamic feature separating the low-lying western coastal plains from the elevated plateau (average elevation ~1 km) characterising the western peninsular India (Fig. 1). The region is covered with a thick pile of lava flows associated with the Deccan volcanism, a consequence of the passage of Indian plate over the Reunion hot spot ~65 million years ago (Duncan and Pyle 1988). Geophysical datasets acquired in the past few decades show that the thickness of the Deccan Traps in the region varies from a few hundred meters to 2 km (Kailasam et al. 1976; Kaila et al. 1981). Recent scientific drilling at 10 sites in the Koyna seismogenic zone provide direct information of Deccan trap thickness in the range 412–1251 m (Roy et al. 2013; Gupta 2017; Roy 2017). A number of lineaments have been mapped from satellite imageries in the region and a few hundred kilometres long, linear belt of hot springs is located along a near coast-parallel (NNW-SSE) alignment, to the west of the Koyna seismogenic zone (Chaterjee and Guha 1968). The 1967 (M6.3) earthquake is associated with a NNE-SSW striking fault, known as the Donichawadi fault, located ~7 km SSE of Koynanagar town (GSI 1968), The earthquake was characterised by a left lateral strike-slip mechanism but the dip of the fault plane (ESE or WNW) remained uncertain (Gupta et al. 1999). The dip of the fault plane was earlier inferred from geological observations near the 905 m hill (near the epicentre) where landslides along NNE striking slip surfaces were found to dip at ~55° towards WNW, and later supported by shallow drilling investigations in the fault zone that suggested ~60° WNW dip of the fault (Gupta et al. 1999).

Fig. 1 Seismicity data (solid circles) of the Koyna-Warna region (Source: Shashidhar et al. 2019) plotted on a topographic map. The events are classified according to their magnitude (circle size) and depth (colour shade) as indicated in the legend. Locations of the GPS sites reported by Gahalaut et al. (2018) (blue solid triangles) and profiles AB, K1K2 and W1W2 (blue solid lines) considered in the present study are shown in the map. Two distinct seismic zones, Koyna Seismic Zone (KSZ) and Warna Seismic Zone (WSZ) are also shown as a shaded rectangular region in the map. Important local faults and lineaments of the area are also superimposed over the map
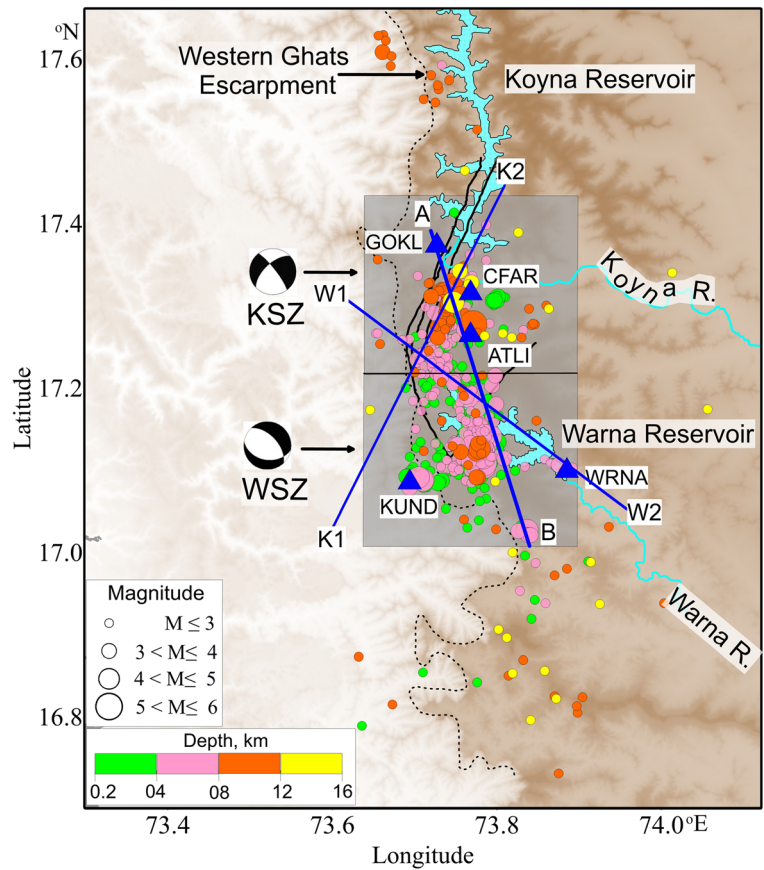

The seismicity of the Koyna-Warna region has been studied extensively by various researchers and over the years, 22 earthquakes of M >5, around 200 earthquakes of M >4 and several thousands of smaller magnitude earthquakes have been reported in the region (Gupta 2017 and references therein). A notable feature is that the seismic activity is confined within ~20×30km^2 area. Two sets of faults have been inferred from study of the focal mechanisms of local events and they are consistent with the local tectonic lineaments (Rao and Shashidhar 2017). Earthquakes closer to the Koyna reservoir show dominantly strike-slip component striking along NNE-SSW direction, whereas, earthquakes nearer to the Warna reservoir show normal faulting mechanism with the strike direction along NW-SE trend (Rao and Shashidhar 2017). Thus, the seismicity distribution delineates two distinct sub-zones, the Koyna Seismic Zone (KSZ) and Warna Seismic Zone (WSZ), which are together referred to as the Koyna-Warna seismic zone (Fig. 1). The majority of earthquakes closer to the

Warna reservoir are located to the depth range 1–8 km whereas those in the vicinity of the Koyna reservoir are found to extend up to 10 km, with a few hypocentres going down to 15 km (Fig. 2).

3 Data and methods

In the present study, published GPS field velocity data of the Koyna-Warna seismic zone (Gahalaut et al. 2018) are used to estimate the strain rates. The estimated strain rates are used to compute the geodetic moment rate, and the strain release rate is estimated based on the seismological catalogues of Shashidhar et al. (2019) and ISC. The gross strain estimates are used to infer the seismic potential of the Koyna-Warna region. Seismic hazard scenario for the potential event has been assessed using stochastic simulation technique. The techniques adopted are summarised below.

Fig. 2 Depth distribution of earthquakes in the Koyna-Warna region, projected along the profile AB (see Fig. 1); the GPS stations are also projected over AB and labeled
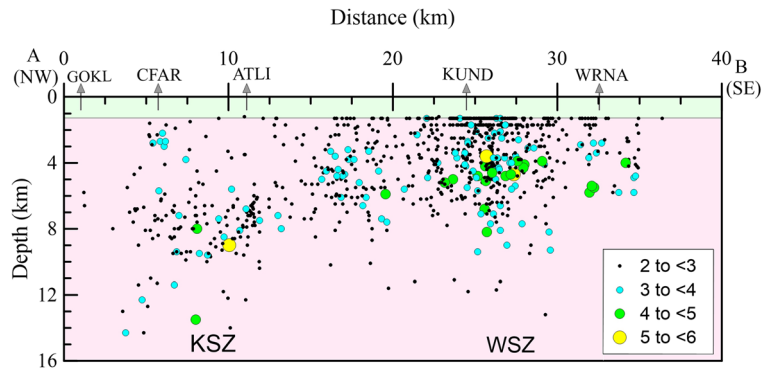
3.1 Estimation of strain rates using GPS velocity

The deformation at a GPS site, given its initial location (x_0, y_0), can be written as,

$$\begin{bmatrix} v_x \\ v_y \end{bmatrix} = \begin{bmatrix} \varepsilon_{xx} & \varepsilon_{xy} - \Omega \\ \varepsilon_{xy} + \Omega & \varepsilon_{yy} \end{bmatrix} \begin{bmatrix} x_0 \\ y_0 \end{bmatrix} + \begin{bmatrix} t_x \\ t_y \end{bmatrix} \quad (1)$$

where v_x is the east velocity and v_y is the north velocity of the GPS site. t_x and t_y are the translational velocities. Ω is the rotational-velocity and ε_{xx}, ε_{xy} and ε_{yy} are the infinitesimal strain rates. Thus, strain rates can be obtained using observed GPS velocities following Cardozo and Allmendinger (2009).

3.2 Elastic dislocation modelling

First-order information on the slip rate and locking depth of any fault zone can be obtained following elastic half space dislocation model as described by Savage and Burford (1973). The model predicts the deformation due to a vertical dislocation of infinite length, buried in a semi-infinite elastic medium. According to this model, the fault parallel velocity v at a distance 'x' perpendicular to the fault trace is given by,

$$v(x) = \frac{S}{\pi} \left[tan^{-1} \left(\frac{x}{D} \right) \right], \quad (2)$$

where D is thickness of the locked zone, S is slip rate and x is distance from the fault. If the fault plane is not perpendicular to the free surface of the earth, the fault plane will introduce an asymmetry in the model and the surface displacement due to a screw dislocation for such inclined fault plane is given by Cohen (1999) and Sandwell (2001)

$$v(x) = \frac{S}{\pi} \left[tan^{-1} \left(\frac{x \, cos^2 \propto}{D' - x \, sin \propto cos \propto} \right) - \propto \right] \quad (3)$$

where $D' = D/cos(\propto)$, $\propto$ is the dip angle, D is the thickness of the locked zone and S is the slip rate.

3.3 Estimation of geodetic moment rate

The maximum of the strain rate data is used to determine the geodetic moment rate ($M_{geodetic}$) of Koyna-Warna region using Kostrov's (1974) formula:

$$M_{geodetic} = 2\mu A H_s e_m \quad (4)$$

where μ is the shear rigidity, H_s is the curstal thickness of the seismogenic zone, A is the surface area over which strain is distributed and e_m is the maximum principal strain component.

3.4 Strain release rate

The moment M_o released by the active fault can be expressed as

$$Mo = \mu DA \quad (5)$$

where $\mu = 3.3*10^{11}$ dyne-cm, D is the displacement of an active fault and A is the rupture area.

The average rate of moment release (r) during an arbitrary duration time t can be obtained as

$$r = \sum M_o / t \quad (6)$$

Total moment released is given by

$$mo = r*t \quad (7)$$

where r is the moment release rate and t is the time period. Mo can be obtained from the equation given by Hanks and Kanamori (1979).

3.5 Stochastic simulation of ground motion

The ground motion has been simulated using stochastic finite fault modelling technique by Motazedian and Atkinson (2005), who introduced the concept of dynamic corner frequency. In this approximation, corner frequency is assumed to be a function of time, i.e. during an earthquake, the rupture begins with a higher corner frequency and progresses to lower corner frequency as the area of rupture grows. The simulation technique involves division of a large fault into numbers of sub-faults, where each sub-fault is considered as a small point source, and the ground motion contributed by each sub-fault is computed and summed at the observation point, with appropriate time delay to obtain the ground motion from the entire fault.

4 Data analysis and results

4.1 Strain rates

GPS field velocities of 5 permanent stations (Fig. 3 and Table 1) are collected from the study by Gahalaut et al. (2018) for the computation of strain parameters using the standard triangulation technique (Cardozo and Allmendinger 2009). The velocity field with respect to the Indian frame of reference is used for the estimation of strain parameters. A total of $^5C_3$ (10) combinations of possible triangles are formed for the computation of strain. Out of the 10 triangles, three triangles are rejected as the interior angles between the stations that formed the triangles were less than 5°. As suggested by Cardozo and Allmendinger (2009), the station combinations that are mostly colinear are rejected for stable estimation of strain. The estimated strain parameters are assigned at the centre of the triangle, as shown in Fig. 3 and listed in Table 2. The centre of the triangles (# 1–5), listed in Table 1, falls close to the KSZ (Fig. 1), whereas, the centre of the remaining three triangles falls in the close proximity of WSZ (Figs. 1 and 3).

4.2 Dislocation modelling

GPS field velocities are projected along parallel and perpendicular directions to the Koyna and Warna fault zones (Fig. 4a and b). It is evident from the figure that small variation in velocity change was observed for the fault parallel and perpendicular projection of GPS velocities along the WSZ. However, a significant velocity change has been observed for KSZ (Fig. 4). Thus, best-fitting elastic model for the study area was obtained for KSZ only with a left lateral slip of 0.8mm/year and dip angle of the fault zone is estimated to be 77° in NW direction. The locking depth of fault zone can be constrained by using dense GPS sites on either side of the fault zone (Smith-Konter et al. 2011). However, we have only 5 observation points in the study area, which are insufficient to resolve the locking depth. The obtained fault dip is however consistent with the results obtained by other geophysical methods (Gupta et al. 1999; Rao and Shashidhar 2017).

4.3 Geodetic moment rates

The geodetic moment ($M_{geodetic}$) rate is estimated using Kostrov's formula (Eq. 4) (Kostrov 1974). In the present case, the area of the source zone (A) is considered to be ~20×30 km² (Gupta 2017) as the seismicity of the Koyna-Warna region is bounded within this area and H_s is the crustal thickness. H_s for the Koyna and Warna regions are reported to vary between 38.6 and 42.3 km with an average of ~40km, which was estimated using the receiver function analysis (Rohilla et al. 2018). Kaila et al. (1981) reported the depths to the Moho discontinuity varying from 31.5km in the west coast to 39km near the Koyna region based on the deep seismic sounding method. Thus, an average crustal thickness H_s of 40 km is considered for the computations in the present study. The average shear modulus of this region is taken to be ~34 GPa, based on in situ measurements in the crystalline basement down to 3-km depth in the Koyna area (Goswami et al. 2017). The estimated $M_{geodetic}$ for seven stations are given in Table 3. Average values for Koyna and Warna regions are considered as ~2.55E+ 16Nm/year and ~2.29E+15Nm/year respectively. Assuming the estimated geodetic moment rate to remain constant after the 1967 M6.3 event due to absence of similar large earthquakes in the region, the KSZ would have accumulated enough strain (strain accumulation rate × time) to generate an earthquake of $M_w6.2$ (Table 4).

4.4 Moment released

The accumulated moment, which gets released in the form of earthquakes in the Koyna-Warna region, is estimated using the available earthquake catalogue of

Fig. 3 Map showing the individual triangles, each formed by joining three GPS stations, for implementing the triangulation technique. GPS stations are marked by blue triangles. The centre of each triangle is marked with a black dot. Extension and compression are marked by the diverging and converging arrows, respectively. The KSZ and WSZ (see Fig. 1) are also shown by shaded regions in the map
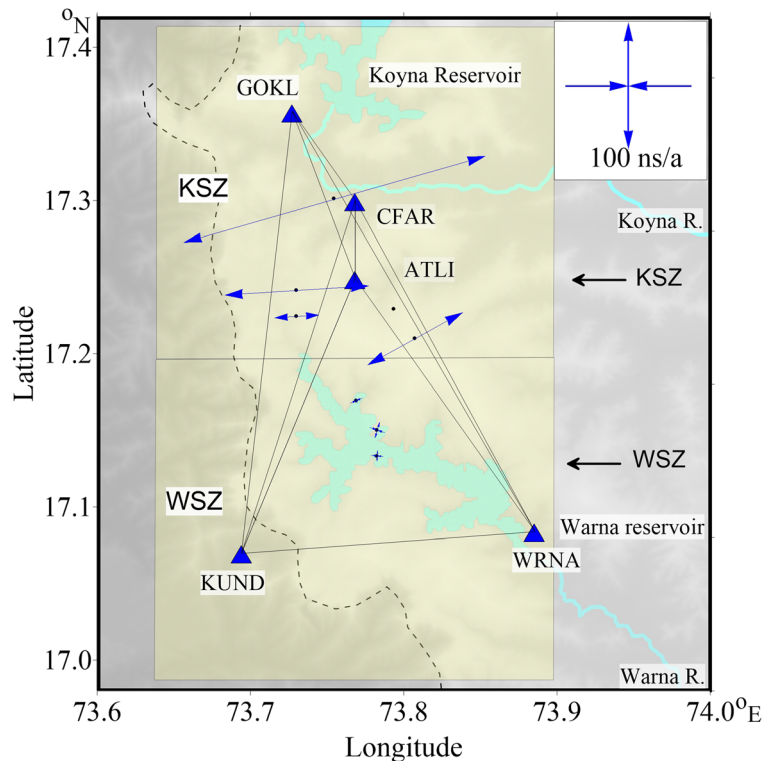
the study area. The recent earthquake catalogue given by Shashidhar et al. (2019) is available for a short period 2005 to 2017, only. Thus, seismic energy release estimates using this catalogue would be based on the events during 2005–2017 only. Therefore, to estimate the total moment released after the 1967 earthquake in Koyna and Warna region separately, we make use of the catalogue published by ISC (www.isc.ac.uk) for the period 1967–2020. The ISC catalogue provides a compilation of event locations and magnitudes for the complete period 1967–2020 and allows us to compare the characteristics of KSZ and WSZ even though the individual

event locations may not be as precise as those obtained using local area networks. Based on the analysis, it is found that the strain energy release rate for the KSZ is ~5.80E+15 Nm/year while that for the WSZ is ~3.30 E+15 Nm/year.

4.5 Radiated energy

The radiated energy for both the source zones, KSZ and WSZ, is also estimated using the earthquake catalogue of the region following the procedure given by Kanamori (1983) using the formula $E=Mo/(2\times10^4)$,

Table 1 Velocity of Indian plate with respect to ITRF 2008 and Indian Reference Frame recorded at five GPS stations in the Koyna-Warna region (Gahalaut et al. 2018)

#	Site	Latitude (°N)	Longitude (°E)	ITRF 2008		Indian Reference Frame	
				V_N (mm/y)	V_E (mm/y)	V_N (mm/y)	V_E (mm/y)
1	WRNA	17.123	73.885	34.4 ± 0.09	40.2 ± 0.07	0.1	0.3
2	CFAR	17.339	73.768	34.1 ± 0.05	39.8 ± 0.04	0.3	0.7
3	ATLI	17.288	73.768	33.9 ± 0.05	39.5 ± 0.04	0.2	0.4
4	GOKL	17.397	73.727	33.8 ± 0.05	39.1 ± 0.04	0.1	0.0
5	KUND	17.109	73.694	33.7 ± 0.07	39.7 ± 0.0	0.0	0.5

Table 2 Strain parameters for Koyna-Warna region estimated using standard triangulation technique

#	Stations forming the triangle			Centre of triangle		E1 (nanostrain)	E2 (nanostrain)	Azimuth of E2 (in degree)	Rotation (nanoradian)	Dilation (nanostrain)	Region to which the centre belongs
				Longitude (°E)	Latitude (°N)						
1	ATLI	CFAR	WARNA	73.807	17.250	88.03	−0.17	243.3	−17.3	87.85	Koyna
2	GOKL	ATLI	CFAR	73.754	17.341	255.45	1.18	255.4	10.2	256.63	Koyna
3	KUND	GOKL	CFAR	73.729	17.281	118.55	−2.34	266.6	36.4	116.21	Koyna
4	KUND	GOKL	ATLI	73.729	17.264	37.05	0.18	266.7	22.1	37.23	Koyna
5	KUND	CFAR	WRNA	73.782	17.190	13.00	−13.13	198.0	−3.5	−0.13	Warna
6	KUND	ATLI	WRNA	73.782	17.173	8.51	−9.90	185.0	2.7	−1.38	Warna
7	KUND	GOKL	WRNA	73.768	17.209	4.447	−10.67	159.4	9.7	−6.22	Warna

where E is the energy in Joules and Mo is the seismic moment in Nm. We have used the catalogue published by Shashidhar et al. (2019) to infer the present-day energy release scenario in the region. Initially, different regression relations of the stable continental region are taken for the conversion of M_L to M_w (Johnston 1996; Schulte and Mooney 2005; Kolathayar and Sitharam 2012), and the average of the estimated M_w is later used to find the energy released using the formula given by Kanamori (1983). The spatial variation of energy is estimated by dividing the region into 0.05°×0.05° grid and the events located within the grid are collected to estimate the energy released in Joules (J). The average

energy is estimated for the collected events and the mean value is assigned at the centre of the rectangular grid. A contour map is then prepared to show the spatial variation of the energy released for the Koyna-Warna region (Fig. 5a). Similarly, the temporal variation in cumulative energy is also estimated for the KSZ and WSZ separately by collecting the events for the respective source zones (Fig. 5a) and the cumulative energy release is plotted for the period (2005–2017) in Fig. 5b The spatial variation of energy also shows that WSZ has released a maximum amount of energy $\sim4.4\times10^{12}$J, whereas for the KSZ, it is $\sim8\times10^{11}$J.
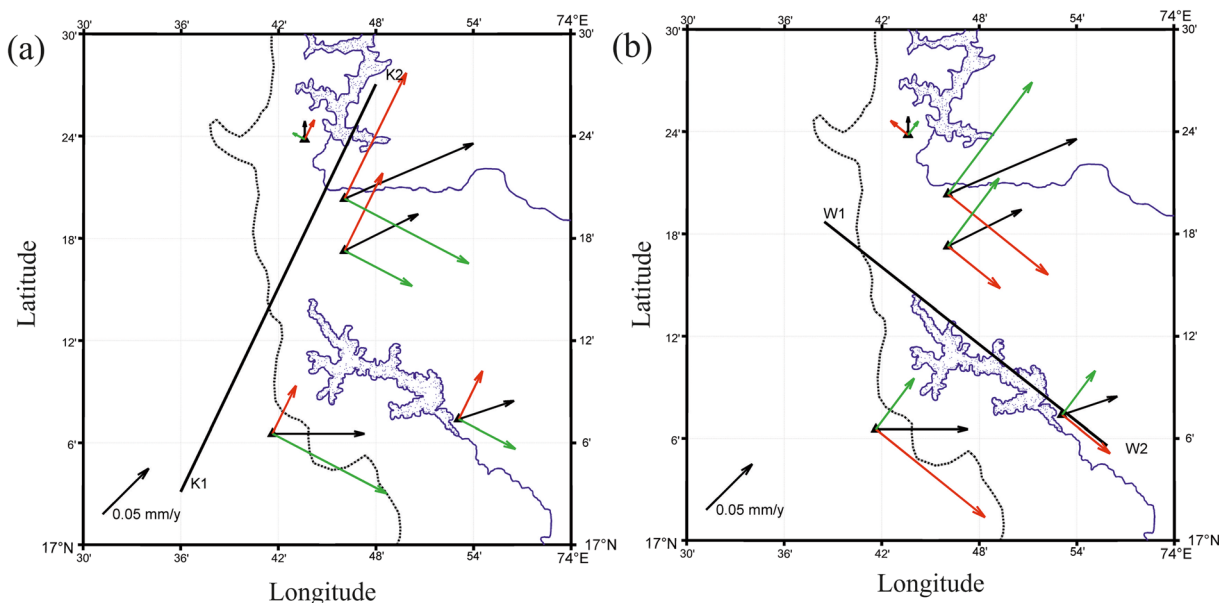
Fig. 4 Velocity components resolved along strike parallel (red arrows) and strike normal (green arrows) directions of the KSZ (**a**) and WSZ (**b**)

Table 3 Geodetic moment rates for Koyna-Warna region

#	Stations forming the triangle			Centre of the triangle		Region to which the centre falls	Geodetic moment rate (Nm/y)	Expected (M_w/y)	Average (M_w/y)
				Longitude (°E)	Latitude (°N)				
1	ATLI	CFAR	WARNA	73.807	17.250	KSZ	1.80E+16	4.8	4.8
2	GOKL	ATLI	CFAR	73.754	17.341	KSZ	5.21E+16	5.1	
3	KUND	GOKL	CFAR	73.730	17.282	KSZ	2.42E+16	4.9	
4	KUND	GOKL	ATLI	73.730	17.265	KSZ	7.56E+15	4.5	
5	KUND	CFAR	WRNA	73.782	17.190	WSZ	2.68E+15	4.2	4.2
6	KUND	ATLI	WRNA	73.782	17.173	WSZ	2.02E+15	4.1	
7	KUND	GOKL	WRNA	73.769	17.210	WSZ	2.18E+15	4.2	

4.6 Gross strain and potential event

Based on the strain budget estimates computed in the present study, KSZ appears to be accumulating more strain energy while releasing the stored energy at a lower rate. If we assume that the energy release rate is constant in the Koyna region since the occurrence of 1967 earthquake (due to absence of any large magnitude event), then Koyna region has released ~3.13E+17Nm of accumulated strain energy post-1967 earthquake, which is only ~23% of the stored strain energy that accumulated (1.38E+18Nm) post-1967 earthquake and the remaining strain is now capable of producing an earthquake equivalent to magnitude M_w~5.8 (Table 4). It can be also noted that the strain energy release rate of WSZ is much higher (~1.4 times) compared to the energy accumulation rate. It may therefore be inferred that the WSZ is not storing enough energy that can produce a large event in near future (Table 4).

4.7 Ground motion simulation

For ground motion simulation, it is assumed that the event may occur at the centre of the KSZ, where seismicity rate is comparatively higher and shows higher energy release (Figs. 1 and 5). Strike of the fault is taken as 207° following the seismicity trend of the KSZ (Fig. 1) and the dip of the fault is taken as 77° as obtained from the dislocation analysis. Event is considered to be located at 10-km depth, following the depth distribution of seismicity of KSZ (Fig. 2). The fault dimension for the M_w5.8 event is obtained from the empirical relations as given by Wells and Coppersmith (1994). Stress drop for the event is assumed to be 90 bars, as source parameter study reveals most of the events in the area falls within the range of 0.03 to 19 MPa with a mean of ~9 MPa (90 bars) (Mandal et al. 1998). The ground motion simulation also requires path and site characteristics at the site of simulation; therefore, site characteristics of hard rock terrains are

Table 4 Strain budget estimates of Koyna-Warna region

E1 (nanostrain)	E2 (nanostrain)	Azimuth of E2 (in degree)	Region to which the centre belongs	Geodetic moment rate (Nm/y)	Accumulated since 1967 (Nm)	Moment release rate (Nm/y)	Remaining potential (Mw)	Average (Mw)
88.03	−0.17	243.3	KSZ	1.80E+16	9.70E+17	5.8e+15	5.8	5.8
255.45	1.18	255.4	KSZ	5.21E+16	2.81E+18	3.3e+15	6.2	
118.55	−2.34	266.6	KSZ	2.42E+16	1.31E+18		5.9	
37.05	0.18	266.7	KSZ	7.56E+15	4.08E+17		5.3	
13.00	−13.13	198.0	WSZ	2.68E+15	1.45E+17		-	-
8.51	−9.90	185.0	WSZ	2.02E+15	1.09E+17		-	-
4.447	−10.67	159.4	WSZ	2.18E+15	1.18E+17		-	-

Fig. 5 a, b The spatial and temporal variations of radiated energy in the Koyna-Warna region are shown in the map for the period 2005–2017 respectively
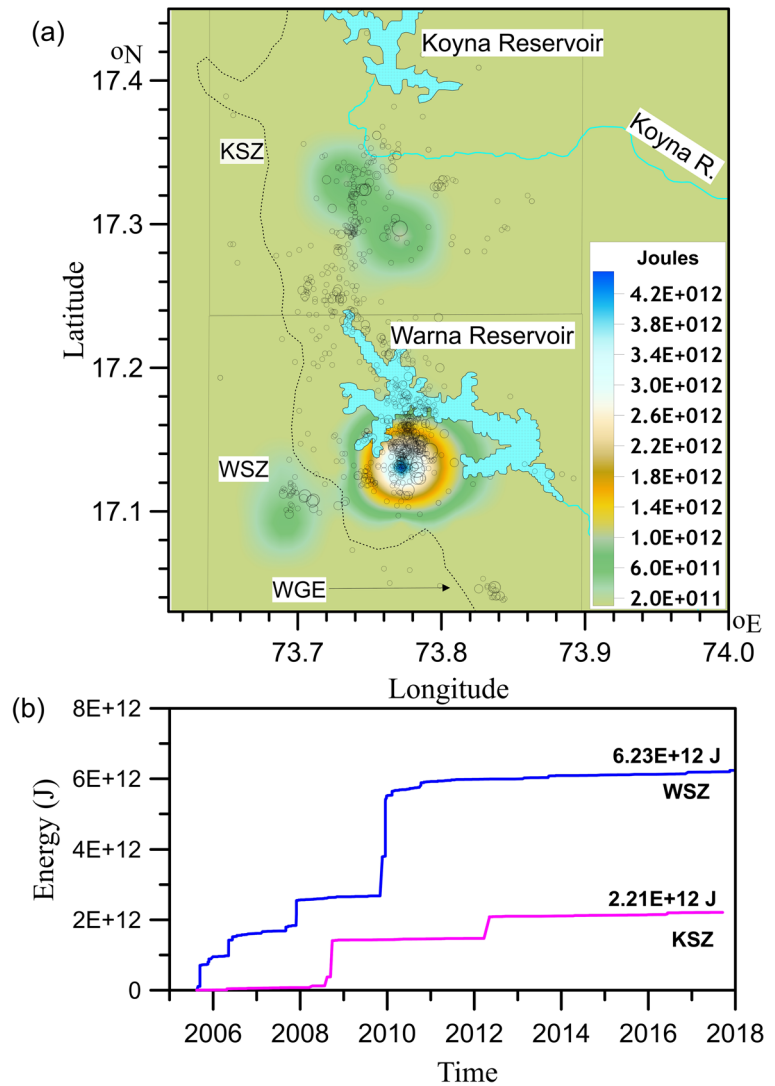
used in the simulation (Atkinson and Boore 2006), as Koyna-Warna region is covered with thick Deccan basalt. The attenuation properties of the medium between the source and the site of stimulation are characterised by the quality factor (Q) and the near-surface attenuation parameter, kappa (k). The seismic wave attenuation parameter (Q) and kappa (k) for the Koyna-Warna region are taken from the published literatures (Sharma et al. 2007; Sairam et al. 2018) and listed in Table 5.

Using the parameters mentioned in Table 5, the ground motion is simulated for the entire Koyna-Warna region at a grid interval of 0.05° using the stochastic simulation technique. The fault is placed at the location 73.764° E and 17.358° N and the top of the fault plane is placed at a depth of 7km. The S-wave velocity and density of the medium are taken to be 3.6 km/s and 2.8 g/cc respectively (Shashidhar et al. 2011). The rupture initiation point is considered as random and a random rupture model is used for simulation. The contour plot of the simulated result is shown in Fig. 6 and the simulated ground motion at selected sites is compared with the available ground motion attenuation relations of the study region (Fig. 7). In general, the simulated PGA follows closely the attenuation curve developed by Iyengar and Raghu Kanth (2004) in the distance range of 10–100 km and supports the simulated ground motion results. The simulated PGA is almost constant or decreasing at a slower rate for the distance range of ~0 to 10 km, which may be due to the consideration of finite fault in the simulation. The available

Table 5 Parameters used in the simulation of M5.8 earthquake

| Parameter	Value	Reference
Strike	207°	This study
Dip	77°	This study
Depth (km)	10	This study
Fault length (km)	11	This study
Fault width (km)	06	This study
Sub-fault along strike	10	This study
Sub-fault along dip	10	This study
Shear wave velocity (km/s)	3.6	Shashidhar et al. 2011
Crustal density (g/cm^3)	2.8	Shashidhar et al. 2011
Stress drop (bars)	90	Mandal et al. 1998
Q	$72f^{1.32}$	Sharma et al. 2007
Geometrical spreading	1/R (R <100 km) 1/R$^{0.5}$ (R >100 km)	Nath and Thingbaijam 2009
Windowing function	Sargoni-Hart	Saragoni and Hart 1973
Kappa	0.02	Sairam et al. 2018

attenuation relations, however, did not consider fault dimension in the formulation, which lead for the mismatch in observed and synthetic PGA up to a distance of 10km from the source.

5 Discussion

The convergence between tectonic plates is largely accompanied by large earthquakes; however, such relations are not well established for intraplate regions but extensive research in this field are underway (e.g. Gupta 2019; Vallage and Bollinger 2019). Earthquakes are manifestations of the release of strain energy, which is accumulated for several years until it exceeds the strength of the medium (Reid 1910). Thus, strain budget estimates of Koyna-Warna region will shed light on the earthquake processes as well as seismic potential of the region.

Strain rate estimates of the study region show that the most extensional strain component is oriented along ENE-WSW direction for the sites close to the KSZ, whereas, the most extensional strain component for the sites in the proximity of WSZ is directed along NNE-SSW direction (Fig. 3). The present-day tectonic activity depends on the relative magnitude and directions of principal extension and principal compression components (Cronin and Resor 2019). From Table 2, the average of the maximum and minimum principal strain

components for the KSZ is 125 nanostrain (ns) and −0.3ns respectively. The strain rates of KSZ are found to be similar to other tectonically active plate boundary regimes around the world (e.g. Hackl et al. 2009; Aktug et al. 2016) and high dilatational rates are associated with faults that recently experienced earthquakes (Hackl et al. 2009). The large extension and negligible compression suggest strike-slip/normal fault tectonic environment, where faults are oriented ≤ 45° to the minor axis of the strain ellipse (Cronin and Resor 2019). Evidently in Fig. 1, a seismicity trend oriented in NNE-SSW direction and striking close to 207° from the north can be observed in the KSZ. In contrast, the WSZ shows the average maximum and minimum strain components to be 8.6 ns and −11.2 ns respectively (Table 2). As both extension and compression components are close to each other, the region is relatively stable compared to the KSZ. The best fitted dislocation model for KSZ shows that the fault dips at 77° and slipping at a rate of 0.8mm/year. It is pertinent to mention here that in the dislocation model, the fault length is assumed to have infinite length and buried in a semi-infinite elastic medium. The infinite length is assumed due to simplicity of antiplane symmetry, which facilitates only non-zero displacement parallel to fault and varies only in the direction perpendicular to fault (Segall 2010). However, actual faults are finite in length, but the technique has been successfully applied to many a fault with different lengths (e.g. Barman et al. 2014; Le Beon
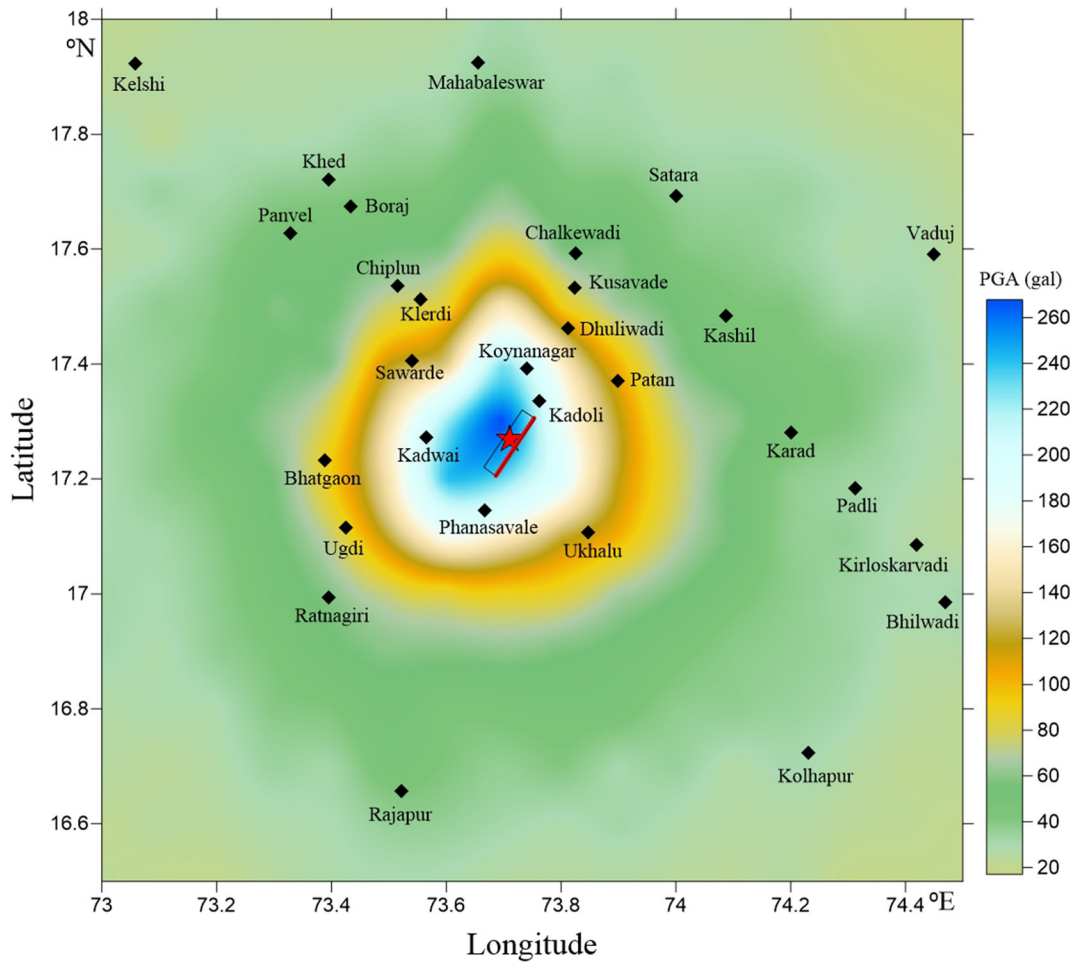
Fig. 6 Simulated peak ground acceleration map (in gals) for a M_w 5.8 earthquake in the Koyna-Warna region at a grid interval of 0.1°. The red star indicates the location of the event. The hypothetical rupture plane of this event is depicted by a black rectangle. Key localities (solid diamonds) in the study region are shown

et al. 2008; Li et al. 2020; Smith-Konter et al. 2011 and many more). In the present study, we used dislocation modelling for a short length fault (< 30 km) within intra-plate setting to get first-hand information about slip rate and locking depth, as slip rate is directly related to seismic potential of a fault (Anderson et al. 1996). The fault dislocation model (Savage and Burford 1973) is utilised only to the KSZ, as a significant change in fault parallel velocities has been perceived for the fault zone and earthquakes in KSZ are strike slip in nature. Both fault parallel and perpendicular velocity components across WSZ are small for the studied time period and earthquakes in WSZ occur mostly with normal fault mechanism (Rao and Shashidhar 2017); therefore, the above-mentioned model is not applied. A 3D model (e.g. Segall 2010), combining both the fault zones,

would be more suitable to obtain more reliable indication of fault slip behaviour for both fault zones, which is a subject of future work.

Furthermore, geodetic strain estimates for the Koyna and Warna region suggest that KSZ is accumulating strain energy at a higher rate (~11 times) in comparison to the WSZ. However, the strain release rate for the WSZ is computed to be higher in comparison to the Koyna region (Table 4). The radiated energy release in the WSZ is also found to be higher, which supports the higher strain release rate for Warna area (Fig. 6a and b). The amount of strain that can accumulate in a region depends on the material properties of that region (Reid 1910). Thus, the estimated higher energy release rate in the WSZ may be attributed to lower strength of the medium properties (e.g. density, elastic constants and
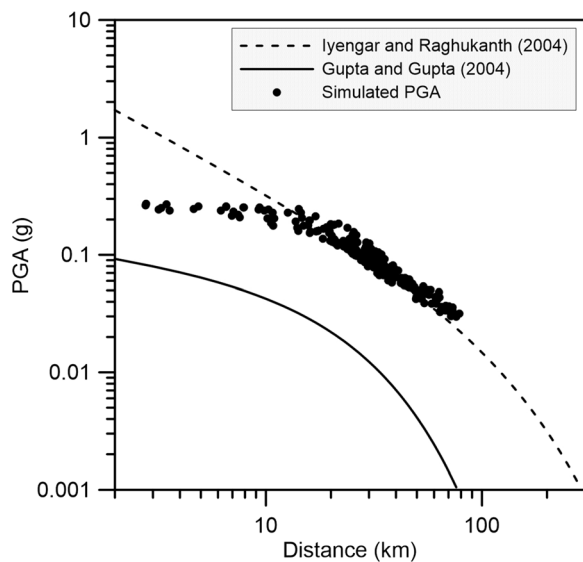
Fig. 7 Variation of PGA (solid circles) with increasing distance from the epicentre of the simulated M5.8 event. Attenuation curves of the Koyna-Warna region, reported by Iyengar and Raghu Kanth (2004) and Gupta and Gupta (2004), are shown

fracture density). Goswami et al. (2017) published Tri-axial test results of core samples collected from four boreholes drilled in the periphery of Koyna-Warna region. Out of the four boreholes, two boreholes located in Phansavle and Kundi are located close to WSZ, whereas the rest boreholes in Nayari and Panchgani are closer to KSZ. Cohesive strength of core samples of Nayari and Panchgahni shows relatively higher value as compared to the rest. Similarly, the co-efficient of internal friction for the samples collected from Phansavle and Kundi shows relatively higher value compared to the sites located closer to the KSZ. Thus, relative variation in material strength can be observed for both the sites.

Furthermore, a refined density structure of the region was collected by high-resolution airborne gravity gradiometry and magnetic data at 1.25-km line spacing over the Koyna-Warna region as part of a multi-parametric geophysical study in the region. An integrated model is developed by combining constraints from seismological, magnetotelluric and borehole data. The recorded gravity gradients are simultaneously inverted to derive density variations down to ~15-km depth. The 3D integrated model has augmented the knowledge of sub-basalt composition, geometry of basement structures and thickness of basalt cover for the region. Concentration of seismicity was also noted at the interfaces of the density anomalies. A cross-section from the 3D sub-surface model along the profile AB is plotted in Fig. 8, which shows relatively high-density values over the Koyna seismic zone compared to the Warna seismic zone, which is also inferred by other researchers (Tiwari and Mishra 1999; Tiwari et al. 2001).

Gupta (2019) suggested that RTS in the Koyna region shall continue for another 2–3 decades due to absence of M~5 magnitude earthquakes in the area. The results obtained in the present study also suggest that the seismicity in the KSZ may continue for a longer time due to higher strain accumulation and slower energy release rates but it may diminish in the WSZ in the near future due to slower strain accumulation and higher release rates.

Strain in the crust is produced due to applied force. The dominant tectonic force closer to the Koyna-Warna region is the ridge push force by the Carlsberg ridge to the west of Koyna-Warna region (Yadav and Tiwari 2018). As Koyna-Warna seismic zone has a dimension of 20×30 km^2, the ridge push force must be applied uniformly to both the KSZ and WSZ at the rate of $\sim 1.9 \times 10^{12}$ N/m (Jayalakshmi and Raghukanth 2016). Thus, significant non-uniformity in the observed strain rates may be associated with variations in the material

Fig. 8 Variation of density distribution along the profile AB (in Fig. 1) obtained from airborne gravity gradiometry (AGG). Depth distribution of earthquakes in the Koyna-Warna region is also projected over the same profile
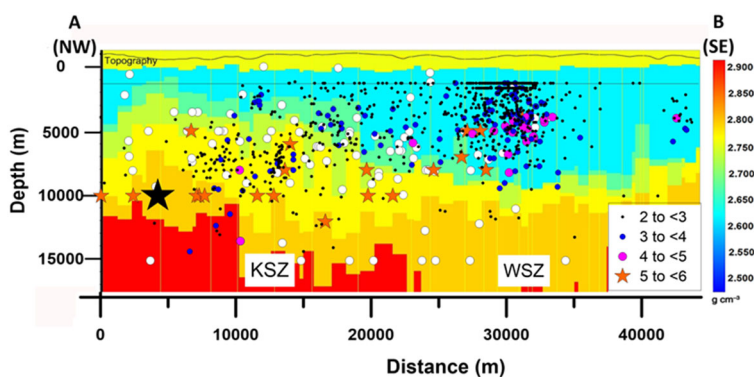
properties or the presence of existing faults and lineaments of the study region.

Based on the above strain budget estimates, we find that the KSZ has accumulated enough potential to date that is capable of generating an earthquake equivalent to $M_w5.8$. The hazard scenario due to occurrence of such event is assessed using the stochastic simulation technique. The simulated ground motion for the Koyna region using selected parameters (Table 5) shows that the source zone may witness strong ground shaking of ~0.26g (Fig. 6) near to the source zone. Places, located at a distance < ~40 km from the source zone such as Ugdi, Bhatgaon, Phanasavale, Ukhalu, Patan, Kadoli, Koynanagar and Sawarde, might witness significant PGA ranging between ~0.09 and ~0.21g. By comparing with the standards of BIS (2002), the places located within a 40-km radius from the source may be associated with intensity between V and VII. Alternatively, the stored energy in the KSZ could be released in multiple low-magnitude events.

6 Conclusions

The estimated rates of strain accumulation as well as strain release for the Koyna-Warna intraplate region suggest a strong spatial variation in the medium properties such as density, elastic constants and fracture density which may exist in the region. Strain measurements further suggest that the KSZ poses a higher seismic hazard in comparison to WSZ. Elastic dislocation modelling for KSZ reveals left lateral slip of 0.8mm/year and the fault zone dips at ~77° in NW direction. Based on gross strain estimates, it is inferred that KSZ can generate an earthquake equivalent to $M_w5.8$, provided the stored energy is released in a single event. Our studies indicate that seismic activity in the WSZ may diminish with time in the near future, whereas, the KSZ may continue to release strain energy in the form of low-magnitude earthquakes for a much longer time. Occurrence of a similar event as that of the $M_w5.8$ earthquake in the Koyna region may produce a strong ground acceleration between 0.09 and 0.26g within ~40-km radius from the source zone.

References

Aktug B, Ozener H, Dogru A, Sabuncu A, Turgut B, Halicioglu K, Yilmaz O, Havazli E (2016) Slip rates and seismic potential on the East Anatolian Fault System using an improved GPS velocity field. J Geodyn 94–95:1–12. https://doi.org/10.1016/j.jog.2016.01.001

Anderson JG, Wesnousky SG, Stirling MW (1996) Earthquake size as a function of fault slip rate. Bull Seismol Soc Am 86: 683–690

Atkinson GM, Boore DM (2006) Earthquake ground-motion prediction equations for Eastern North America. Bull Seismol Soc Am 96(6):2181–2205. https://doi.org/10.1785/0120050245

Barman P, Ray JD, Kumar A, Chowdhury JD, Mahanta K (2014) Estimation of present-day inter-seismic deformation in Kopili fault zone of north-east India using GPS measurements. Geom Nat Hazards Risk 5705(2):1–14. https://doi.org/10.1080/19475705.2014.983187

BIS (2002) Indian standard criteria for earthquake resistant design of structure. Part 1 resistant provision and buildings. Bureau of Indian Standards, New Delhi

Cardozo N, Allmendinger RW (2009) SSPX—a program to compute strain from displacement/velocity data: Computers and Geosciences, 35, 1343–1357. https://doi.org/10.1016/j.cageo.2008.05.008

Chaterjee GC, Guha SK (1968) The problem of origin of high temperature springs of India. Proc Symp (II), 23rd Int Geol Cong, Prague 17:141–149

Cohen SC (1999) Numerical models of crustal deformation in seismic zones. Adv Geophys 41:134–231

Cronin V, Resor P (2019) GPS and infinitesimal strain analysis, GETSI's Earth-focused Modules for Undergraduate Classroom and Field Courses, https://serc.carleton.edu/168230. Accessed November 2020

Duncan RA, Pyle DG (1988) Rapid eruption of Deccan flood basalts at the Cretaceous/Tertiary boundary. Nature 333: 841–843

G.S.I (1968) A geological report on the Koyna earthquake of 11 the December, 1967, Satara District, Maharashtra State. Report submitted by Officers of the Geological Survey of India, March 1968, 273.

Gahalaut VK, Gahalaut K, Joshi KC, Sreejith KM, Agrawal R, Yadav RK, Mohanalakshmi CH, Naidu MS, Rao VR (2018) Geodetic constraints on tectonic and anthropogenic deformation and seismogenesis of Koyna–Warna region, India. Bull Seismol Soc Am 108(5B):2933–2942

Goswami D, Akkiraju V, Misra S, Roy S, Singh SK, Sinha A, Gupta H, Bansal BK, Nayak S (2017) Rock strength measurements on Archaean basement granitoids recovered from scientific drilling in the active Koyna seismogenic zone, western India. Tectonophysics:712–713

Guha SK, Gosavi PD, Varma M, Agarwal SP, Padale JG, Marwadi SC (1968) Recent seismic disturbances in the Koyna Hydroelectric Project, Maharashtra, India. Report, Central Water and Power Research Station, India

Gupta HK (2017) Koyna, India, an ideal site for near field earthquake observations. J Geol Soc India 90:645–652

Gupta HK (2019) Koyna, India, an ideal site for near field earthquake observations. Proc Indian Natn Sci Acad 85 No 2:469–480. https://doi.org/10.1007/S12594-017-0771-2

Gupta S, Gupta ID (2004) The prediction of earthquake peak ground acceleration in Koyna region, India, 13th World Conference on Earthquake Engineering, Vancouver, B.C., Canada, Paper No. 1437

Gupta H, Narain H, Rastogi BK, Mohan I (1969) A study of the Koyna earthquake of December 10, 1967. Bull Seismol Soc Am 59(3):1149–1162

Gupta HK, Rao RUM, Srinivisan R, Rao GV, Reddy GK, Dwivedy KK, Banerjee DC, Mohanty R, Satyasaradhi YR (1999) Anatomy of surface rupture zones of two stable continental region earthquakes, 1967 Koyna and 1993 Latur. India Geophys Res Lett 26(13):1985–1988

Hackl M, Malservisi R, Wdowinski S (2009) Strain rate patterns from dense GPS networks. Nat Hazards Earth Syst Sci 9: 1177–1187. https://doi.org/10.5194/nhess-9-1177

Hanks TC, Kanamori H (1979) A moment magnitude scale. J Geophys Res 84(5):2348–2350. https://doi.org/10.1029/JB084iB05p02348

IS 1893 (1962) Recommendations for earthquake resistant design of structures. Bureau of Indian Standards, N Delhi

Iyengar RN, Raghu Kanth STG (2004) Attenuation of strong ground motion in peninsular India. Seismol Res Lett 75(4): 530–540. https://doi.org/10.1785/gssrl.75.4.530

Jayalakshmi S, Raghukanth STG (2016) Intra plate stresses using finite element modelling. Acta Geophys 64:1370–1390. https://doi.org/10.1515/acgeo-2016-0050

Johnston AC (1996) Seismic moment assessment of earthquakes in stable continental regions- instrumental seismicity: Geophys. J Int 124:381–414

Kaila KL, Reddy PR, Dixit M, Lazarenko M (1981) Deep crustal structure of Koyna, Maharashtra indicated by deep seismic soundings. J Geol Soc India 22:1–16

Kailasam LN, Reddy AGB, Joga Rao MV, Satyamurthy YK, Murthy BPR (1976) Deep electrical resistivity soundings in the Deccan Trap region. Curr Sci 45:9–13

Kanamori H (1983) Magnitude scale and quantification of earthquakes. Tectonophysics 93:185–199

Kolathayar S, Sitharam TG (2012) Characterization of regional seismic source zones in and around India. Seismol Res Lett 83(1):77–85

Kostrov BV (1974) Seismic moment and energy of earthquakes and seismic flow of rock. Izvestiya-Physics of the Solid Earth 1:23–40

Le Beon M, Klinger Y, Amrat AQ et al (2008) Slip rate and locking depth from GPS profiles across the southern Dead Sea Transform. J Geophys Res Solid Earth 113:11403. https://doi.org/10.1029/2007JB005280

Li J, Zhou B, Li T, Yang Y, Li Z (2020) Locking depth, slip rate, and seismicity distribution along the Daofu–Kangding segment of the Xianshuihe fault system, eastern Tibetan Plateau. J Asian Earth Sci 193:104328. https://doi.org/10.1016/j.jseaes.2020.104328

Mandal P, Rastogi BK, Sarma CSP (1998) Source parameters of Koyna earthquakes, India. Bull Seismol Soc Am 88(3):833–842

Milne J (1911) A catalogue of destructive earthquakes A.D. 7 to A.D. 1899. British Association for the Advancement of Science, Portsmouth, 1911, p 92

Motazedian D, Atkinson GM (2005) Stochastic finite-fault modeling based on a dynamic corner frequency. Bull Seismol Soc Am 95:995–1010

Narain H, Gupta HK (1968) Koyna earthquake. Nature. 217: 1138–1139

Nath SK, Thingbaijam KKS (2009) Seismic hazard assessment: a holistic microzonation approach. Nat Hazards Earth Syst Sci 9:1445–1459. https://doi.org/10.5194/nhess-9-1445-2009

Rao NP, Shashidhar D (2017) Earthquake focal mechanism studies in Koyna-Warna region in the last five decades - Current understanding on tectonics and seismogenesis. J Geol Soc India 90:684–691. https://doi.org/10.1007/s12594-017-0776-7

Rastogi BK, Chadha RK, Sarma CSP, Mandal P, Satyanarayana HVS, Raju IP, Kumar N, Satyamurthy C, Nageswara Rao A (1997) Seismicity at Warna reservoir (near Koyna) through 1995. Bull Seismol Soc Am 87(6):1484–1494

Reid HF (1910) The mechanics of the earthquake, The California Earthquake of April 18, 1906, report of the State Investigation Commission, vol 2. Carnegie Institution of Washington, Washington, D.C.

Rohilla S, Ravi Kumar M, Rao NP, Satyanarayana HVS (2018) Shear-wave velocity structure of the Koyna–Warna region, Western India, through modeling of P-receiver functions. Bull Seismol Soc Am 108(3A):1314–1325

Roy S (2017) Scientific drilling in Koyna region, Maharashtra. Curr Sci 112(11):2181–2181

Roy S, Rao NP, Akkiraju VV, Goswami D, Sen M, Gupta HK, Bansal BK, Nayak S (2013) Granitic basement below Deccan traps unearthed by drilling in the Koyna Seismic zone, Western India. J Geol Soc India 81:289–290

Sairam B, Singh AP, Ravi Kumar M (2018) Comparison of earthquake source characteristics in the Kachchh Rift Basin and Saurashtra horst, Deccan Volcanic Province, western India. J Earth Syst Sci 127:55

Sandwell DT (2001) Elastic solutions for strike-slip faulting. Unpublished class note, https://topex.ucsd.edu/geodynamics/. Accessed June 2021

Saragoni GR, Hart GC (1973) Simulation of artificial earthquakes. Earthq Eng Struct Dyn 2(3):249–267. https://doi.org/10.1002/eqe.4290020305

Savage JC, Burford RO (1973) Geodetic determination of relative plate motion in central California. J Geophys Res 78:832–845

Schulte SM, Mooney WD (2005) An updated global earthquake catalogue for stable continental regions—reassessing the correlation with ancient rifts. Geophys J Int 161:707–721

Segall P (2010) Earthquake and volcano deformation. Princton University Press, p 456

Sharma B, Teotia SS, Kumar D (2007) Attenuation of P, S, and coda waves in Koyna region. India J Seismol 11:327–344. https://doi.org/10.1007/s10950-007-9057-z

Shashidhar D, Rao NP, Gupta HK (2011) Waveform inversion of broad-band data of local earthquakes in the Koyna–Warna region, western India. Geophys J Int 185(1):292–304

Shashidhar D, Mallika K, Mahato C, Maity BS, Sudheer K, Satyanarayana HVS, Purnachandra Rao N, Raghavan RV, Sarma ANS, Murthy YVVBSN, Gowri Shankar U, Narsingarao D, Uma Anuradha M (2019) A catalogue of earthquakes in the Koyna-Warna region, Western India (2005–2017). J Geol Soc India 93:7–24. https://doi.org/10.1007/s12594-019-1115-y

Smith-Konter BR, Sandwell DT, Shearer P (2011) Locking depths estimated from geodesy and seismology along the San Andreas fault system: implications for seismic moment release. J Geophys Res 116:B0640

Tiwari VM, Mishra DC (1999) Estimation of effective elastic thickness from gravity and topography data under the Deccan volcanic province, India, Earth planet. Sci Lett 171: 189–299

Tiwari VM, Rao MBSV, Mishra DC (2001) Density inhomogeneities beneath Deccan volcanic province, India as derived from gravity data. J Geodyn 31:1–17

Vallage A, Bollinger L (2019) Testing fault models in intraplate settings: a potential for challenging the seismic hazard assessment inputs and hypothesis? Pure Appl Geophys 177: 1879–1889. https://doi.org/10.1007/s00024-019-02129-z

Wells DL, Coppersmith KJ (1994) New empirical relationships among magnitude, rupture length, rupture width, rupture area, and surface displacement. Bull Seismol Soc Am 84(4):974–1002

Yadav R, Tiwari VM (2018) Numerical simulation of present-day tectonic stress across the Indian subcontinent. Int J Earth Sci 107:2449–2462. https://doi.org/10.1007/s00531-018-1607-9

Publisher's note   Springer Nature remains neutral with regard to jurisdictional claims in published maps and institutional affiliations.